Modelling a broad class of actuator saturations using Takagi-Sugeno models with a reduced number of local models

Gustave Bainier[1], Benoît Marx[1], Jean-Christophe Ponsart[1]

***Abstract*— In this paper, the Takagi–Sugeno (T-S) models are suggested as modelling tools to represent both the behavior of a nonlinear system and its saturated actuators. Given a T-S system with r local models, previous works on input saturation usually required $2^{n_u}r$ or $3^{n_u}r$ local models to represent an actuator saturated outside of an orthotope (n_u stands for the input vector dimension). In this paper, an elementary representation is suggested, which only takes $2r$ local models (thus, independently of n_u), and is able to capture a much broader class of actuator saturations. Local stabilization conditions expressed as linear matrix inequalities (LMI) are provided using the conventional static parallel distributed compensation (PDC) state feedback scheme. A heuristic solution is given in order to ensure a large guaranteed domain of attraction. Numerical examples are given in order to demonstrate the proposed approach and initiate a discussion on its contributions and limitations.**

I. Introduction

In control engineering, actuator saturation is a common type of constraint on the control inputs of a physical plant, which arises from the impossibility of applying unbounded control signals, usually because of material limitations or safety requirements. This phenomenon introduces a nonlinearity in the system which can significantly reduce its closed-loop performance and potentially cause instability. Hence, the saturation has to be accounted for in the design of a controller. Two main strategies exist in the literature in order to design a controller subject to saturation [1].

The first strategy involves a two-step process. First, a nominal controller is developed without considering the actuator saturation; then, an anti-windup compensator is designed to handle the saturation constraint. This compensator computes the discrepancy between the unsaturated and the saturated control signals and retroactively uses it to modify the pre-designed controller [2]. This approach is ordinarily adopted in linear settings, and only a few extensions exists for Takagi-Sugeno (T-S) systems (e.g. [3]–[5]).

In the second strategy, the saturation constraints are incorporated right from the start of the design process. Various methods have been developed using this approach, including the set invariance framework, which ensures that any state trajectory starting within an invariant set remains bounded inside it, preventing states from exceeding known bounds [1]. However, guaranteeing a large domain of attraction with this approach is often obtained by imposing constraints on the feedback gains, which hinders the performances of the controllers designed to prevent saturation (e.g. [6]–[8]).

[1]Université de Lorraine, CNRS, CRAN, F-54000 Nancy, France gustave.bainier@univ-lorraine.fr

The T-S community usually deals with saturation the set invariance framework with a polytopic representation approach, and merges it with gain scheduling (e.g. [7]–[11]). These techniques, which this paper focuses on, leverage - explicitly or implicitly - the nonlinear sector approach (NLSA, also called sector nonlinearity transformation) to represent both the nonlinear system and its saturated actuators within a T-S framework [12]. Unfortunately, in a typical T-S fashion, this leads to a large number of submodels and generates optimization problems with a lot of LMI, limiting their applicability. In particular, given a T-S system with r local models and an input vector u of dimension n_u, $2^{n_u}r$ ([7]–[10] etc) or $3^{n_u}r$ ([11]) local models are needed to represent u saturated outside of an orthotope. Moreover, these existing T-S techniques are not only difficult to grasp intuitively, painful to compute, but also limited in their intrinsic modelling capabilities: what if u is saturated outside of a polytope, or any other convex shape ?

This paper mitigates the disadvantages of the T-S approach to actuator saturation by obtaining a flexible representation which captures a broad class of actuator saturations. The representation discussed in this paper leverages the Minkowski functional associated with the saturating set, and only demands $2r$ local models, no matter the geometry of the saturating set or the dimension of u. This leads to a reduced number of LMI in the local stabilization conditions, hence simplifying and reducing the conservatism of the approach. Moreover, a heuristic method is given to increase the chances of obtaining a large guaranteed domain of attraction, while explicitly allowing saturation to happen (as in [11]). Despite these advantages, this method comes with a few drawbacks: guaranteeing a minimal size for the domain of attraction does not come with a simple and generic solution, and - in the orthotopic case - the lack of "component-wise decomposition" of the saturated input vector may lead to a smaller domain of attraction than previous approaches. Numerical simulations are given in order to point out the contributions of the proposed method, as well as to quantify its shortcomings.

This paper is organized as follows: Section II introduces the notations used in the paper. In Section III, the Minkowski functional is presented as a crucial tool to derive a simple and exact T-S representation of a saturating actuator. Section IV provides a local stabilization technique for the previously introduced T-S model by employing a saturated PDC controller, and details a heuristic method to maximize the guaranteed domain of attraction. In Section V, practical insights on the proposed method are presented through

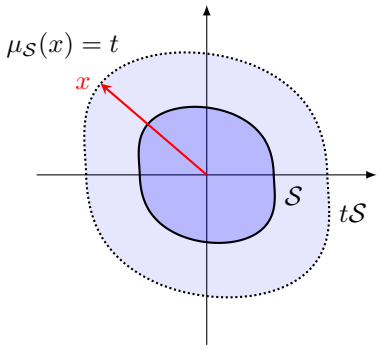

Fig. 1. Minkowski functional of a set $\mathcal{S}$ of $\mathbb{R}^2$ evaluated at x

numerical simulations. Finally, Section VI concludes the paper.

II. Notations

$\mathbb{R}$ stands for the set of real numbers, $\mathbb{R}_{\geq 0} \triangleq \{x \in \mathbb{R}, x \geq 0\}$, $\mathbb{R}_{>0} \triangleq \{x \in \mathbb{R}, x > 0\}$ and $\overline{\mathbb{R}}_{\geq 0} = \mathbb{R}_{\geq 0} \cup \{+\infty\}$. $\mathbb{R}^{p\times q}$ stands for the set of real matrices with p rows and q columns. $\mathbb{R}^{p\times 1}$ is identified with the Euclidean space $\mathbb{R}^p$ with its usual inner product $\langle\cdot|\cdot\rangle$. Given a matrix $E \in \mathbb{R}^{p\times q}$, $E^\top$ denotes its transposition, and if $p = q$, then $\mathcal{H}(E) = E^\top + E$. Given two symmetric matrices $E, F \in \mathbb{R}^{p\times p}$, $E \succ F$ means that $E - F$ is positive-definite (which is denoted $E - F \succ 0$) and that $F - E$ is negative-definite ($F - E \prec 0$). I_n stands for the identity matrix of $\mathbb{R}^{n\times n}$. Let $\mathcal{S}$ denote a subset of $\mathbb{R}^n$, $\mathrm{int}(\mathcal{S})$, $\mathrm{cl}(\mathcal{S})$ and $\partial\mathcal{S}$ denote respectively the interior, the closure and the boundary of $\mathcal{S}$ in $\mathbb{R}^n$.

III. T-S modeling of the saturation

In this section, the Minkowski functional is introduced as a useful tool to represent through a single scalar value the saturation level of a vector compared to a convex saturating set. First, the definition of the Minkowski functional is provided together with its expression for common convex sets and some of its established properties. Then, it is leveraged to obtain an exact T-S representation of an actuator saturating outside of a convex set.

A. The Minkowski functional

Intuitively, the Minkowski functional $\mu_{\mathcal{S}}$ associated with the set $\mathcal{S} \subset \mathbb{R}^n$ is defined such that for all $x \in \mathbb{R}^n$, $\mu_{\mathcal{S}}(x)$ provides the smallest scaling t of the set $\mathcal{S}$ with respect to the origin such that the scaled set $t\mathcal{S} \triangleq \{ty : y \in \mathcal{S}\}$ reaches x (Figure 1). This definition is formalized below, and the expression of the Minkowski functional is specified for usual classes of convex sets.

Definition 1 (Minkowski functional [13]): Given $\mathcal{S}$ a non-empty set of $\mathbb{R}^n$, the Minkowski functional associated to $\mathcal{S}$ is the map $\mu_{\mathcal{S}} : \mathbb{R}^n \to \overline{\mathbb{R}}_{\geq 0}$ defined by:

$$\mu_{\mathcal{S}}(x) \triangleq \inf\{t \in \overline{\mathbb{R}}_{\geq 0} : x \in t\mathcal{S}\} \tag{1}$$

Example 1 (p-Ball [13]): The Minkowski functional of $\mathcal{B}_p \subset \mathbb{R}^n$ the unit ball of norm p centered at the origin is given by:

$$\mu_{\mathcal{B}_p}(x) = \|x\|_p \tag{2}$$

where $\|x\|_p$ stands for the p-norm of x.

Example 2 (Ellipsoid [14]): The Minkowski functional of an ellipsoid $\mathcal{E} \subset \mathbb{R}^n$ centered at the origin is given by:

$$\mu_{\mathcal{E}}(x) = \mu_{M\mathcal{B}_2}(x) = \sqrt{x^\top Q x} \tag{3}$$

with $M \in \mathbb{R}^{n\times m}$ a full row rank matrix, and $Q = Q^\top \succ 0$ the positive definite matrix given by $Q = (MM^\top)^{-1}$.

Example 3 (Polytope [15]): Given $\mathcal{P} \subset \mathbb{R}^n$ a closed and convex polytope whose interior contains the origin and whose halfspace-representation is given by:

$$\mathcal{P} = \{x \in \mathbb{R}^n : \forall k \in [\![1, m]\!],\ \langle h_k|x\rangle \leq 1\} \tag{4}$$

with $(h_k)_{1\leq k\leq m}$ as set of m vectors of $\mathbb{R}^n$, then, the Minkowski functional of $\mathcal{P}$ is given by:

$$\mu_{\mathcal{P}}(x) = \max_{k\in[\![1,m]\!]} \langle h_k|x\rangle \tag{5}$$

Example 4 (Radially parameterized set): Given $\mathcal{O} \subset \mathbb{R}^n$ a star-convex set at 0 whose boundary can be parameterized radially by the continuous map $\rho : [0, \pi)^{n-2}\times[0, 2\pi) \to \mathbb{R}_{>0}$ such that

$$\partial\mathcal{O} = \left\{ \rho(\varphi_1, \ldots, \varphi_{n-1}) \begin{bmatrix} \cos\varphi_1 \\ \sin\varphi_1\cos\varphi_2 \\ \vdots \\ \sin\varphi_1 \ldots \sin\varphi_{n-2}\cos\varphi_{n-1} \\ \sin\varphi_1 \ldots \sin\varphi_{n-2}\sin\varphi_{n-1} \end{bmatrix} \right\} \tag{6}$$

with $(\varphi_1, \ldots, \varphi_{n-1}) \in [0, \pi)^{n-2} \times [0, 2\pi)$, then the Minkowski functional of $\mathcal{O}$ is given by:

$$\mu_{\mathcal{O}}(x) = \frac{\|x\|_2}{\rho(\varphi_1, \ldots, \varphi_{n-1})} \tag{7}$$

where $\varphi_1, \ldots, \varphi_{n-1}$ stand for the following angular coordinates of x:

$$\forall k \in [\![1, n-2]\!], \varphi_k = \arccos \frac{x_k}{\sqrt{\sum_{i=k}^n x_i^2}} \tag{8a}$$

$$\varphi_{n-1} = 2\,\mathrm{arccot}\, \frac{x_{n-1} + \sqrt{x_n^2 + x_{n-1}^2}}{x_n} \tag{8b}$$

The classical properties on the Minkowski functional associated with a convex set are recalled hereafter.

Property 1 (Convex properties [13]): If $\mathcal{S}$ is convex and $0 \in \mathrm{int}(\mathcal{S})$:

1) For all $x \in \mathbb{R}^n \setminus \{0\}$, $0 < \mu_{\mathcal{S}}(x) < +\infty$, $\mu_{\mathcal{S}}(0) = 0$,
2) For all $x \in \mathbb{R}^n$ and $t \in \mathbb{R}_{\geq 0}$, $\mu_{\mathcal{S}}(tx) = t\mu_{\mathcal{S}}(x)$, and $\mu_{\mathcal{S}}(tx) = \mu_{\frac{1}{t}\mathcal{S}}(x)$ if $t \neq 0$,
3) For all $x_1, x_2 \in \mathbb{R}^n$, $\mu_{\mathcal{S}}(x_1 + x_2) \leq \mu_{\mathcal{S}}(x_1) + \mu_{\mathcal{S}}(x_2)$
4) $\mu_{\mathcal{S}}$ is a continuous map from $\mathbb{R}^n$ to $\mathbb{R}_{\geq 0}$
5) $\mu_{\mathcal{S}}^{-1}([0, 1)) = \mathrm{int}(\mathcal{S})$, $\mu_{\mathcal{S}}^{-1}([0, 1]) = \mathrm{cl}(\mathcal{S})$, $\mu_{\mathcal{S}}^{-1}(\{1\}) = \partial\mathcal{S}$

B. T-S model of a convex saturation

The T-S model (9) is presumed to represent a nonlinear system subject to actuator saturation outside of $\mathcal{S} \subset \mathbb{R}^{n_u}$, a convex set containing the origin in its interior ($0 \in \mathrm{int}(\mathcal{S})$).

$$\dot{x}(t) = \sum_{i=1}^r h_i(\theta)[A_i x(t) + B_i u_{\mathcal{S}}(t)] \tag{9}$$

In this model, $x(t) \in \mathbb{R}^{n_x}$ stands for the state vector, $u_{\mathcal{S}}(t) \in \mathcal{S} \subset \mathbb{R}^{n_u}$ stands for the saturated input vector, r denotes the number of local models, and $\theta \in \mathbb{R}^{n_\theta}$ is a vector of scheduling parameters assumed to be known in real-time. The activation functions $(h_i)_{1\leq i\leq r}$ satisfy the convex sum properties:

$$h_i(\theta) \geq 0, \qquad \sum_{i=1}^{r} h_i(\theta) = 1 \tag{10}$$

The T-S model (9) can easily be rewritten as (11) with an unrestricted input vector $u(t) \in \mathbb{R}^{n_u}$, using the map $u \mapsto \text{act}(u)u$, guaranteeing a continuous mapping from $\mathbb{R}^{n_u}$ to $\mathcal{S}$:

$$\dot{x}(t) = \sum_{i=1}^{r} h_i(\theta)[A_i x(t) + \text{act}(u(t))B_i u(t)] \tag{11}$$

with act : $\mathbb{R}^{n_u} \to (0, 1]$ the continuous scalar map defined by:

$$\text{act}(u) = \begin{cases} 1 & \text{if } \mu_{\mathcal{S}}(u) \leq 1 \\ 1/\mu_{\mathcal{S}}(u) & \text{if } \mu_{\mathcal{S}}(u) > 1 \end{cases} \tag{12}$$

Continuity is indeed obtained from the 4th item of Property 1. This rewriting is powerful, since it reduces all the nonlinearities induced by the saturation of u to a bounded scalar term pre-multiplying the input matrices B_i. From here, an exact representation of (11) is obtained.

Theorem 1 (Open-loop T-S rewriting): Let $\tau \in [0, 1)$ and $\mathcal{U}_\tau \triangleq \{u \in \mathbb{R}^{n_u} : \text{act}(u) \geq \tau\}$. For all $u \in \mathcal{U}_\tau$, the T-S model (13) is an exact representation of (11).

$$\dot{x}(t) = \sum_{i=1}^{r} \sum_{k=1}^{2} h_i(\theta) h_k^\tau(u(t))[A_i x(t) + B_{i,k} u(t)] \tag{13}$$

with $B_{i,1} = B_i$, $B_{i,2} = \tau B_i$ and:

$$h_k^\tau(u) = \begin{cases} (\text{act}(u) - \tau)/(1 - \tau) & \text{if } k = 1 \\ (1 - \text{act}(u))/(1 - \tau) & \text{if } k = 2 \end{cases} \tag{14}$$

Proof: Since $\text{act}(u) \in [\tau, 1]$, (14) follows from the NLSA [12]. ∎

Remark 1: For all $\tau \in (0, 1)$, (13) only represents (11) locally ($\mathcal{U}_\tau \subset \mathbb{R}^{n_u}$). However, for $\tau = 0$, (13) is a global representation of (11) ($\mathcal{U}_0 = \mathbb{R}^{n_u}$).

IV. Saturated PDC state feedback control law

This section investigates the local stabilization of the saturated T-S model (9) controlled by (15), a PDC state feedback [16] employing the same activation functions as in (9).

$$u_{\mathcal{S}}(t) = \text{act}(u(t))u(t) \text{ with } u(t) = \sum_{i=1}^{r} h_i(\theta) K_i x(t) \tag{15}$$

Remark 2: The parameters of the activation functions are now denoted implicitly, i.e. h_i stands for $h_i(\theta)$ and h_k^τ stands for $h_k^\tau(u(t))$.

Remark 3: In a similar context, the T-S literature has already considered a PDC feedback law which involves the activation functions $(h_k^\tau)_{k=1,2}$ [8]. However, this gives rise to a self-referential effect in which the control signal $u(t)$ depends on its own current value. Indeed, the simulations of [8] do not employ these activation functions.

A. LMI conditions for stabilization using PDC state feedback

As a direct consequence of Theorem 1, injecting (15) within the T-S system (13) provides an exact representation of the closed-loop system [12].

Lemma 1 (Closed-loop T-S rewriting): For a given $\tau \in [0, 1)$ and

$$\mathcal{X}_\tau \triangleq \left\{ x \in \mathbb{R}^{n_x} : \mu_{\mathcal{S}} \left(\sum_{i=1}^{r} h_i K_i x \right) \leq \frac{1}{\tau} \right\} \tag{16}$$

(if $\tau = 0$, $\mathcal{X}_0 = \mathbb{R}^{n_x}$). For all $x \in \mathcal{X}_\tau$, the T-S model (17) is an exact representation of (9) taken with the control law (15).

$$\dot{x}(t) = \sum_{i=1}^{r} \sum_{j=1}^{r} \sum_{k=1}^{2} h_i h_j h_k^\tau [A_i + B_{i,k} K_j] x(t) \tag{17}$$

From this representation, the following local stabilization conditions, expressed as LMI, can be obtained.

Theorem 2 (Local Stabilization Conditions): Let $\mathcal{E}_{\lambda^*} \triangleq \{x \in \mathbb{R}^n : x^\top P x \leq \lambda^*\}$ denote the biggest ellipsoid contained within the set $\mathcal{X}_\tau$. The T-S model (9) taken with the control law (15) is guaranteed to be exponentially stable on $\mathcal{E}_{\lambda^*}$ if there exists $X = X^\top \succ 0$ and $(M_j)_{1\leq j\leq r}$ such that:

$$\sum_{i=1}^{r} \sum_{j=1}^{r} h_i h_j \mathcal{H} \left[A_i X + B_i M_j \right] \prec 0 \tag{18a}$$

$$\sum_{i=1}^{r} \sum_{j=1}^{r} h_i h_j \mathcal{H} \left[A_i X + \tau B_i M_j \right] \prec 0 \tag{18b}$$

with $X = P^{-1}$, $M_j = K_j X$.

Proof: Introducing the quadratic Lyapunov function $V(x) = x^\top P x$, the LMI (18a) and (18b) are obtained by applying the results of [17] to the closed loop system (17) resp. for $k = 1, 2$. ∎

Remark 4: If $\tau = 0$, then $\mathcal{E}_{\lambda^*} = \mathbb{R}^{n_x}$, additionally if (18b) has a solution, then the input-free system is already globally exponentially stable.

Remark 5: It is easy to adapt the LMI (18a) to impose a minimum decay rate or a H_∞ attenuation criterion when the controller is not saturating. Identical adaptations can be made to both the LMI (18a) and (18b) to impose similar (but typically less demanding) guarantees up to the saturation level $\text{act}(u) \geq \tau$.

B. Heuristic for an improved numerical implementation

Finding the largest ellipsoid $\mathcal{E}_{\lambda^*}$ contained inside $\mathcal{X}_\tau$ is a hard problem in general, hence optimizing the size of $\mathcal{E}_{\lambda^*}$ through the LMI (18) is a difficult task which could be tackled using computationally heavy derivative free optimization methods. Moreover, the actual domain of attraction for a given set of gains $(K_i)_{1\leq i\leq r}$ can be much larger than $\mathcal{E}_{\lambda^*}$ itself, hence this optimization problem would only maximize the *guaranteed* domain of attraction, and not necessarily

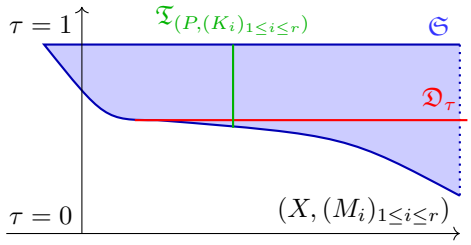

Fig. 2. Schematic illustration of the sets $\mathfrak{T}_{(P,(K_i)_{1\le i\le r})}$, $\mathfrak{D}_\tau$ and $\mathfrak{S}$

the domain of attraction itself. However, our approach has provided a set of LMI (18) which are limited in their number, size, and which are extremely simple to grasp. This leads to a heuristic solution to the problem of maximizing the guaranteed domain of attraction. Three key observations are given below and schematically illustrated in Figure 2:

Observation 1: Let $\mathfrak{T}_{(P,(K_i)_{1\le i\le r})}$ denote the interval of all scalar values of $\tau \in [0,1)$ solving the LMI (18) for fixed Lyapunov function and set of gains $(P,(K_i)_{1\le i\le r})$. Of course, (16) guarantees that the minimal value τ of $\mathfrak{T}_{(P,(K_i)_{1\le i\le r})}$ provides the largest $\mathcal{X}_\tau$ set, which in turns maximizes the guaranteed domain of attraction $\mathcal{E}_{\lambda^*}$.

Observation 2: Let $\mathfrak{D}_\tau$ denote the convex set of all decision variables $(X,(M_i)_{1\le i\le r})$ solving the LMI (18) for a fixed $\tau \in [0,1)$. Well chosen weighted sums of (18b) and (18a) provide that for all $\tau_1,\tau_2 \in [0,1)$ such that $\tau_1 \le \tau_2$, then $\mathfrak{D}_{\tau_1} \subseteq \mathfrak{D}_{\tau_2}$, with the empty set being a subset of every possible set, including itself. Therefore, trying to minimize τ in (18) when $(P,(K_i)_{1\le i\le r})$ are not fixed does not guarantee a larger domain of attraction $\mathcal{E}_{\lambda^*}$, but rather limits the size of the Lyapunov function and feedback gain set from which a solution is picked by the solver.

Observation 3: Let $\mathfrak{S}$ denote the set of all decision variables $(\tau,X,(M_i)_{1\le i\le r})$ solving the bilinear matrix inequalities (BMI) (18) (which is only a set of LMI for a fixed τ). For all $(\tau,X,(M_i)_{1\le i\le r}) \in \mathfrak{S}$ and $\alpha \in \mathbb{R}_{>0}$ it is easily verified that $(\tau,\alpha X,(\alpha M_i)_{1\le i\le r}) \in \mathfrak{S}$. Hence, as long as $\mathfrak{S}$ is not empty, it is unbounded. Moreover, if there also exists $\beta \in (0,1]$ such that $(\tau,X,(M_i/\beta)_{1\le i\le r})$ is a solution to (18a), then $(\beta\tau,X,(M_i/\beta)_{1\le i\le r}) \in \mathfrak{S}$. Intuitively, as long as the stabilizing gains can be scaled up in the unsaturated system, τ can be scaled down accordingly. It can be deduced from (16) and item 2 of Property 1 that this scaling has no effect on the size of $\mathcal{X}_\tau$, hence on the guaranteed domain of attraction $\mathcal{E}_{\lambda^*}$.

Observation 1 indicates that keeping P and $(K_i)_{1\le i\le r}$ relatively "fixed" gives relevance to the pursue of the minimization of τ as a means to maximize the guaranteed domain of attraction $\mathcal{E}_{\lambda^*}$. However, Observation 2 underscores that providing excessive flexibility to these variables diminishes this relevance. This is partly explained by Observation 3, since scaling up the feedback gains can result in a reduced value of τ without any substantial impact on the guaranteed domain of attraction $\mathcal{E}_{\lambda^*}$. Heuristically, it can therefore be conjectured that constraining further the optimization problem to limit this "meaningless scaling effect" should enhance the results obtained by minimizing τ. To this end, it is suggested to impose a *maximum* decay rate $\alpha/2 > 0$ to the unsaturated system, resulting in the following additional LMI to (18):

$$\sum_{i=1}^{r}\sum_{j=1}^{r} h_i h_j \mathcal{H}\left[A_i X + B_i M_j\right] \succ -\alpha X \qquad (19)$$

The purpose of this heuristic is not to enforce a "low decay rate": the objective is to ensure that the solver does not seek large gains *in order* to minimize τ. Large values of α can therefore be taken so the performances of the controller are not compromised. In case of redundant inputs, this heuristic might need to be repeated on a selection of columns of B_i. The effectiveness of this heuristic is investigated numerically in the next section through the measure of the influence of τ on the volume of the guaranteed domain of attraction (20) (Figures 5 and 7)

$$\mathrm{Vol}(\mathcal{E}_{\lambda^*}) = \frac{2\pi^{n_x/2}}{n_x\Gamma\left(n_x/2\right)}\sqrt{\det((P/\lambda^*)^{-1})} \qquad (20)$$

where Γ stands for the usual gamma function [18].

V. Numerical Examples

The LMI problems (18) and (19) are investigated using the relaxation scheme found in [19] with $p = 3$, and solved numerically using MOSEK 10.1 with default settings.

A. Example 1: investigating the maximum decay rate heuristic

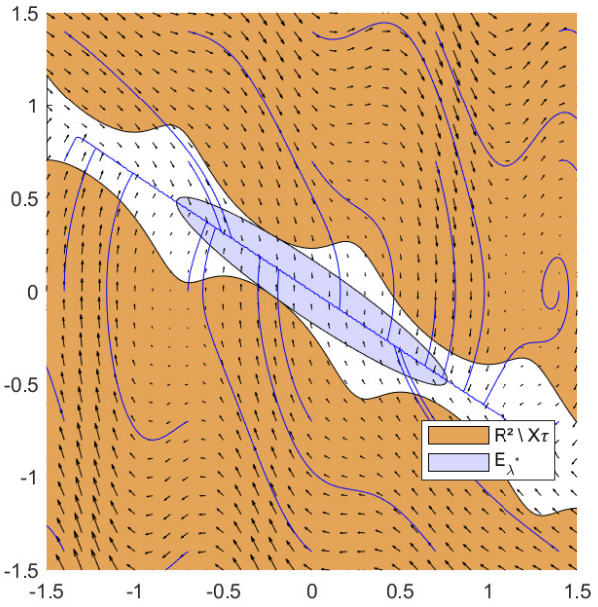

Fig. 3. Closed-loop state space, $\tau = 0.004$, no maximum decay rate α

Consider the following nonlinear second-order system:

$$\ddot{y}(t) = \sin(2\pi y(t))(y(t) + \dot{y}(t)) + u_{\mathcal{S}}(t) \qquad (21)$$

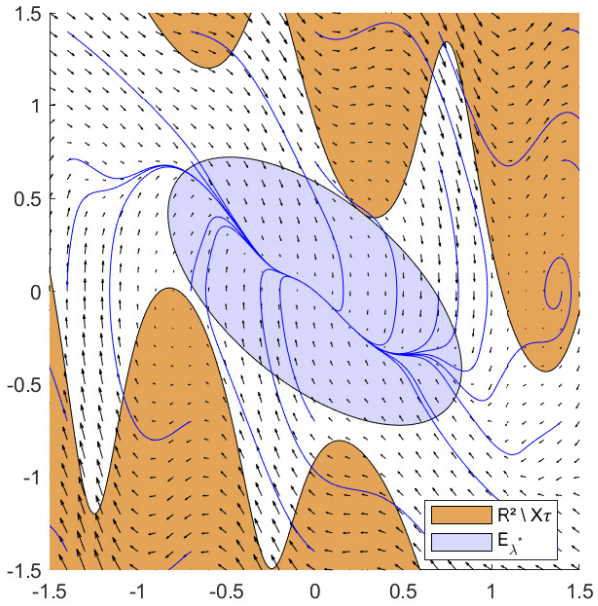

Fig. 4. Closed-loop state space, with minimal $\tau = 0.18$ found for $\alpha = 15$

where the input $u_{\mathcal{S}}(t)$ is saturating outside the set $\mathcal{S} = [-1, 1]$ (which gives $\mu_{\mathcal{S}}(u) = |u|$). This system is rewritten as the exact T-S model (22) using Theorem 1:

$$\dot{x}(t) = \sum_{i=1}^{2}\sum_{k=1}^{2} h_i(\theta)h_k^{\tau}(u(t))[A_i x(t) + B_{i,k}u(t)] \quad (22)$$

with $x = \begin{bmatrix} x_1 & x_2 \end{bmatrix}^\top = \begin{bmatrix} y & \dot{y} \end{bmatrix}^\top$, $\theta = y = x_1$, $u_{\mathcal{S}} = \text{act}(u)u$, $A_1 = \begin{bmatrix} 0 & 1 \\ 1 & 1 \end{bmatrix}$, $A_2 = \begin{bmatrix} 0 & 1 \\ -1 & -1 \end{bmatrix}$, $B_{1,1} = B_{2,1} = \begin{bmatrix} 0 & 1 \end{bmatrix}^\top$, $B_{1,2} = B_{2,2} = \tau B_{1,1}$, and with the following activation functions:

$$h_1(x_1) = (1 + \sin(2\pi x_1))/2, \quad h_2(x_1) = 1 - h_1(x_1) \quad (23)$$

In order to stabilize the system, a PDC state feedback law of the form (15) is calculated at several values of τ through the LMI (18) of Theorem 2, both with and without imposing a maximum decay rate $\alpha/2$ through (19). The closed loop state space of (21) is plotted on Figures 3 and 4 with the "exact region" and guaranteed region of attraction $\mathcal{X}_\tau$ and $\mathcal{E}_{\lambda^*}$ of (22). In both cases, the blue trajectories show an actual region of attraction much larger that the guaranteed one.

Numerically, as long as no maximum decay rate is imposed through the LMI (19), it seems that τ can be chosen arbitrarily in $(0, 1)$ with an unclear effect on the volume of the guaranteed domain of attraction $\text{Vol}(\mathcal{E}_{\lambda^*})$. However, adding a maximum decay rate unambiguously makes the minimization problem of τ relevant to obtain a large volume for the guaranteed domain of attraction, with no clear correlation between the choice of α and the largest value of $\text{Vol}(\mathcal{E}_{\lambda^*})$ (Figure 5).

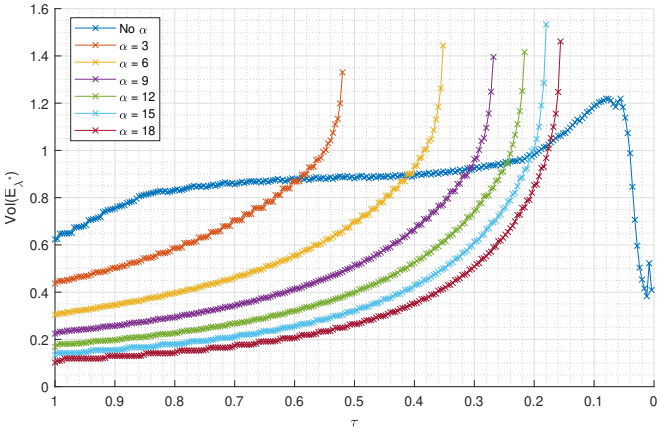

Fig. 5. Volume of the guaranteed domain of attraction $\text{Vol}(\mathcal{E}_{\lambda^*})$ depending on τ at several values of α

B. Example 2: investigating the number of local models

The T-S model (22) is modified so $u(t) \in \mathbb{R}^2$, $\mathcal{S} = [-1, 1]^2$, $A_1 = \begin{bmatrix} 0 & 1 \\ a & b \end{bmatrix}$, $A_2 = \begin{bmatrix} 0 & 1 \\ -a & -b \end{bmatrix}$, $B_{i,1} = I_2$ and $B_{i,2} = \tau I_2$, with $a, b \in \mathbb{R}$. Using the same LMI as previously, but imposing (19) on both columns of $B_{i,1}$ because of the input redundancy, the conservatism of computing a saturated PDC controller is investigated using:

- this paper representation of $\mathcal{S}$ ($2r = 4$ local models),
- the usual literature representation ($2^2 r = 8$ local models).

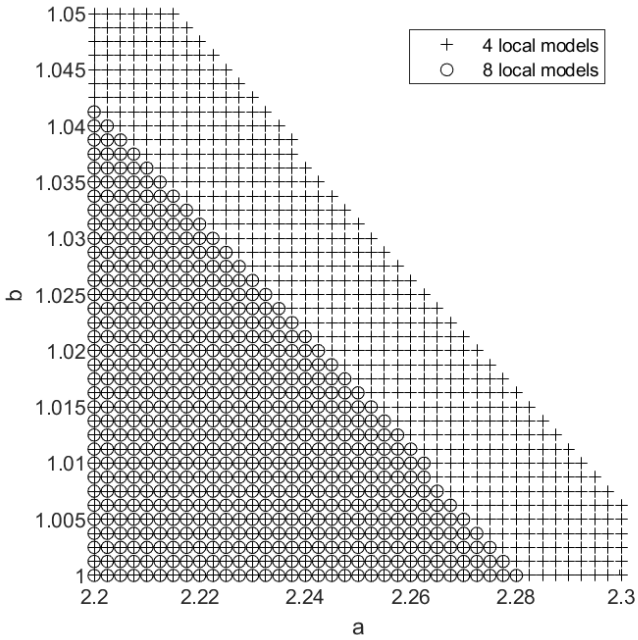

Fig. 6. Feasibility spaces, $\tau = 0.11$, $\alpha = 15$

Fixing $(\tau, \alpha) = (0.11, 15)$, Figure 6 compares for several values of a, b the conservatism of both representations through the feasibility space of the LMI computing a saturated PDC controller. Unsurprisingly, the feasibility space is

larger using the proposed representation with 4 local models than with 8. This was easily anticipated since the LMI problem with 4 local models is included in the LMI problem with 8 local models.

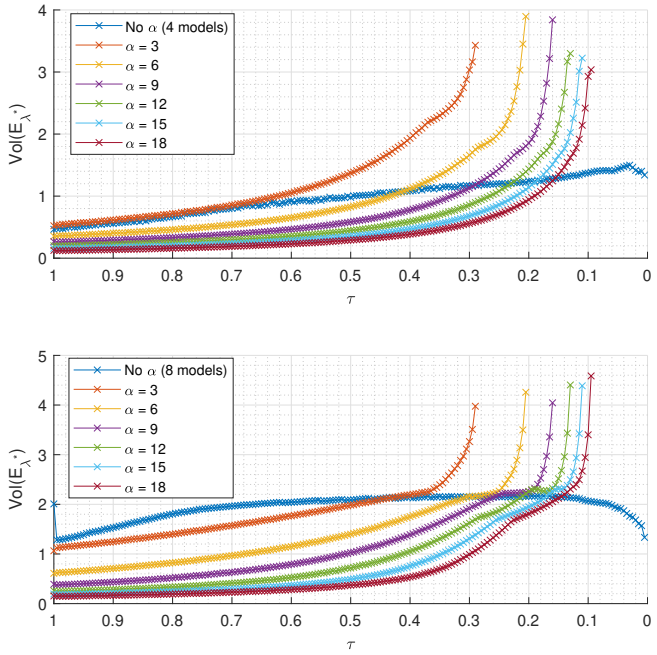

Fig. 7. Volume of the guaranteed domain of attraction $\text{Vol}(\mathcal{E}_{\lambda^*})$ depending on τ at several values of α, with $(a, b) = (2.2, 1)$

Fixing $(a, b) = (2.2, 1)$, Figure 7 investigates the heuristic of imposing (19) to obtain a large domain of attraction. Again, this heuristic tends to make the minimization of τ relevant to obtain a large volume for the guaranteed domain of attraction. However, the improvement is smaller for the T-S system with 8 local models than with 4 local models. It can be conjectured that the multiplication of local models naturally constraints the optimization problem, making the minimization of τ more effective on its own, without having to impose new LMI conditions. It is worth highlighting that the guaranteed domain of attraction is also smaller by using 4 models than 8 models, but this disadvantage needs to be put into perspective: this is not a comparison of the actual domain of attraction, but a comparison of an easily computed theoretical guarantee for the PDC controller.

VI. Conclusions and Perspectives

This paper has presented a novel T-S representation of a large class of saturated actuators by leveraging the Minkowski functional associated with the saturating set. Contrary to previous works which solely considers orthotopic or ellipsoidal saturations, this representation is valid for all convex saturations. Moreover, very few local models are needed, which drastically reduces the number of LMI in the usual local stabilization conditions for a PDC state feedback law. Furthermore, a heuristic method to enhance the chances of achieving a large guaranteed domain of attraction is provided and numerically examined on two examples. This work can easily be expanded to other control law, such as the non-PDC or the output feedback approaches. In the end, guaranteeing a large domain of attraction in the design of a saturated control for a nonlinear system remains a complex issue. Hopefully, this paper opens the way to some new efficient approaches to the problem within the T-S framework.

References

[1] S. Tarbouriech, G. Garcia, J. M. G. da Silva, and I. Queinnec, *Stability and Stabilization of Linear Systems with Saturating Actuators*. Springer London, 2011.

[2] L. Zaccarian and A. R. Teel, *Modern Anti-windup Synthesis: Control Augmentation for Actuator Saturation*. Princeton University Press, 2011.

[3] M. Klug, E. B. Castelan, V. J. Leite, and L. F. Silva, "Fuzzy dynamic output feedback control through nonlinear Takagi-Sugeno models," *Fuzzy Sets and Systems*, vol. 263, pp. 92–111, Mar. 2015.

[4] A. Nguyen, A. Dequidt, and M. Dambrine, "Anti-windup based dynamic output feedback controller design with performance consideration for constrained Takagi-Sugeno systems," *Engineering Applications of Artificial Intelligence*, vol. 40, pp. 76–83, apr 2015.

[5] A. N. D. Lopes, V. J. S. Leite, L. F. P. Silva, and K. Guelton, "Anti-windup TS fuzzy PI-like control for discrete-time nonlinear systems with saturated actuators," *International Journal of Fuzzy Systems*, vol. 22, pp. 46–61, jan 2020.

[6] K. Tanaka and H. O. Wang, *Fuzzy Control Systems Design and Analysis*. Wiley, Sept. 2001.

[7] Y.-Y. Cao and Z. Lin, "Robust stability analysis and fuzzy-scheduling control for nonlinear systems subject to actuator saturation," *IEEE Transactions on Fuzzy Systems*, vol. 11, pp. 57–67, feb 2003.

[8] J. Zhang, W.-B. Xie, M.-Q. Shen, and L. Huang, "State augmented feedback controller design approach for T-S fuzzy system with complex actuator saturations," *International Journal of Control, Automation and Systems*, vol. 15, pp. 2395–2405, Sept. 2017.

[9] D. Saifia, M. Chadli, S. Labiod, and T. M. Guerra, "Robust H_∞ static output feedback stabilization of T-S fuzzy systems subject to actuator saturation," *International Journal of Control, Automation and Systems*, vol. 10, pp. 613–622, jun 2012.

[10] L. Zhao and L. Li, "Robust stabilization of T-S fuzzy discrete systems with actuator saturation via PDC and non-PDC law," *Neurocomputing*, vol. 168, pp. 418–426, nov 2015.

[11] S. Bezzaoucha, B. Marx, D. Maquin, and J. Ragot, "State and output feedback control for Takagi-Sugeno systems with saturated actuators," *International Journal of Adaptive Control and Signal Processing*, vol. 30, pp. 888–905, nov 2015.

[12] G. Bainier, B. Marx, and J.-C. Ponsart, "Generalized nonlinear sector approaches for Takagi-Sugeno models," *Fuzzy Sets and Systems*, vol. 476, p. 108791, Jan. 2024.

[13] D. Luenberger, *Optimization by vector space methods*. New York: Wiley, 1968.

[14] F. Blanchini and S. Miani, "Convex sets and their representation," in *Set-Theoretic Methods in Control*, pp. 93–119, Springer International Publishing, 2015.

[15] M. Fiacchini, C. Prieur, and S. Tarbouriech, "On the computation of set-induced control Lyapunov functions for continuous-time systems," *SIAM Journal on Control and Optimization*, vol. 53, pp. 1305–1327, Jan. 2015.

[16] H. Wang, K. Tanaka, and M. Griffin, "An approach to fuzzy control of nonlinear systems: stability and design issues," *IEEE Transactions on Fuzzy Systems*, vol. 4, no. 1, pp. 14–23, 1996.

[17] D. H. Lee, Y. H. Joo, and M. H. Tak, "LMI conditions for local stability and stabilization of continuous-time T-S fuzzy systems," *International Journal of Control, Automation and Systems*, vol. 13, pp. 986–994, may 2015.

[18] M. Jorgensen, "Volumes of n-dimensional spheres & ellipsoids," 2014.

[19] A. Sala and C. Ariño, "Asymptotically necessary and sufficient conditions for stability and performance in fuzzy control: Applications of Polya's theorem," *Fuzzy Sets and Systems*, vol. 158, no. 24, pp. 2671–2686, 2007.